Journal of Solid State Chemistry 182 (2009) 1581–1586

Contents lists available at ScienceDirect

Journal of Solid State Chemistry

journal homepage: www.elsevier.com/locate/jssc

Synthesis of anatase nanoparticles with extremely wide solid solution range and $ScTiNbO_6$ with α-PbO_2 structure

Masanori Hirano *, Takaharu Ito

Department of Applied Chemistry, Faculty of Engineering, Aichi Institute of Technology, Yakusa, Toyota 470-0392, Japan

ARTICLE INFO

Article history:
Received 5 February 2009
Received in revised form
6 March 2009
Accepted 28 March 2009
Available online 8 April 2009

Keywords:
Anatase
Rutile
α-PbO_2
Phase transition
Solid solution

ABSTRACT

Anatase-type nanoparticles $Sc_XTi_{1-2X}Nb_XO_2$ with wide solid solution range ($X = 0$–0.35) were hydrothermally formed at 180 °C for 5 h. The lattice parameters a_0 and c_0, and the optical band gap of anatase gradually and linearly increased with the increase of the content of niobium and scandium from $X = 0$ to 0.35. Their photocatalytic activity and adsorptivity by the measurement of the concentration of methylene blue (MB) that remained in the solution in the dark or under UV-light irradiation were evaluated. The anatase phase existed stably up to 900 °C for the samples with $X = 0.25$–0.30 and 750 °C for that with $X = 0.35$ during heat treatment in air. The phase with α-PbO_2 structure and the rutile phases coexisted in the samples with $X = 0.25$–0.30 after heated at temperatures above 900–950 °C. The α-PbO_2 structure having composition $ScTiNbO_6$ with possibly some cation order similar to that seen in wolframite existed as almost completely single phase after heat treatment at temperatures 900–1500 °C through phase transformation from anatase-type $ScTiNbO_6$.

1. Introduction

The precipitation technique from aqueous solution under hydrothermal conditions, which is one of the aqueous solution routes, is of current interest [1] and is attractive for the direct formation of crystalline fine ceramic particles. Generally, hydrothermal reactions are carried out in an autoclave at temperature between the boiling and critical points of water at elevated pressure. Fine powders of various oxide ceramics have been prepared via the hydrothermal route because of the excellent homogeneity and uniformity of the synthesized particles [2,3]. From the point of view of saving energy and environmental benignity, hydrothermal synthesis method under small autogenous pressure below about 250 °C, i.e. mild hydrothermal synthesis is suitable for low-temperature preparation of nanophase materials of different sizes and shapes [4–7] and new compound [8,9].

Titanium dioxide has been extensively used as an environmentally harmonious and clean photocatalyst [10] and its modification has also been attempted by doping with various elements. However, to form homogeneous anatase-type TiO_2 solid solutions with dopant through solid-state reaction with heat treatment at 600–1000 °C is not so easy because pure anatase phase is metastable and easily changes to stable rutile one by heat treatment above 635 °C from the result of the kinetic study [11,12]. Thus, mild hydrothermal synthesis methods have been applied to preparation of anatase-type titania solid solutions doped with iron [13], zirconium [14–16], niobium [17,18], scandium [19], and so on. In our previous work, the direct formation of new anatase-type solid-solutions of $Al_XTi_{1-2X}Nb_XO_2$ [20] and $Sc_XTi_{1-2X}Nb_XO_2$ [21] in the range $X = 0$–0.20 was performed via the synthesis of nanocrystalline particles using the mild hydrothermal synthesis. On the other hand, in addition to well-known three distinct polymorphs: rutile, anatase, and brookite, pure titania (TiO_2) can exist as orthorhombic structure (α-PbO_2(scrutinyite)-type) [22–24] and monoclinic baddeleyite-type structure [25] under high pressure.

In the present study, the possibility of the presence of anatase-type solid solution $Sc_XTi_{1-2X}Nb_XO_2$ with wider solid solution range ($X > 0.20$) than that in the previous report [21] was investigated. The photoactivity of thus obtained anatase-type $Sc_XTi_{1-2X}Nb_XO_2$ solid solutions was evaluated separately by the measurement of the concentration of methylene blue (MB) remained in the solution in the dark or under UV-light irradiation. The effects of the amount of dopant materials i.e. the value of X in $Sc_XTi_{1-2X}Nb_XO_2$ on the structure, optical band gap, photocatalytic activity, phase stability of anatase, and phase transformation behavior were investigated. As the results of those investigations, wide solid solution range ($X = 0$–0.35) of anatase-type $Sc_XTi_{1-2X}Nb_XO_2$ nanoparticles were found using mild hydrothermal synthesis technique at 180 °C for 5 h. Furthermore, the presence of a $ScTiNbO_6$ ($= Sc_{0.33}Ti_{0.33}Nb_{0.33}O_2$) compound having α-PbO_2 structure with possibly some cation order similar to that seen in wolframite was discovered through phase transformation from anatase by heat treatment at temperatures above 900 °C.

* Corresponding author. Fax: +81 565 48 0076.
E-mail addresses: hirano@aitech.ac.jp, hirano@ac.aitech.ac.jp (M. Hirano).

0022-4596/$ - see front matter © 2009 Elsevier Inc. All rights reserved.
doi:10.1016/j.jssc.2009.03.020

Table 1
Starting composition and urea concentration of samples and analytical values of chemical composition of as-prepared anatase-type Titania.

Sample	Starting composition (molar fraction)			Urea concentration (mol/dm^3)	Analytical value (molar fraction)			
X	Sc	Ti	Nb		Sc	Ti	Nb	X
0.20	0.200	0.600	0.200	1.40	0.168	0.661	0.171	0.170
0.25	0.250	0.500	0.250	1.50	0.216	0.556	0.229	0.223
0.30	0.300	0.400	0.300	1.60	0.265	0.465	0.270	0.268
0.35	0.350	0.300	0.350	1.70	0.320	0.358	0.322	0.321

2. Experimental

Anatase-type nanoparticles $Sc_XTi_{1-2X}Nb_XO_2$ with starting composition ($X = 0$–0.35) were synthesized under hydrothermal conditions at 180 °C for 5 h as previously reported [21]. The starting composition and the concentration of urea are shown in Table 1. In the present study, the hydrothermally prepared powders were heated at 700–1100 °C for 1 h. The samples were characterized via X-ray diffractometry (XRD), transmission electron microscopy (TEM), an inductivity-coupled plasma emission spectrometer (ICP), the adsorption isotherm of nitrogen at 77 K based on the Brunauer–Emmett–Teller method (BET), the optical absorption (using an ultraviolet–visible spectrophotometer), and estimation of photocatalytic activity and adsorptivity (using change in the concentration of methylene blue, MB) as described in the previous study [21].

3. Results and discussion

3.1. Direct synthesis of anatase-type solid solution nanoparticles

Scandium has most similar ionic radius to titanium in many rare-earth elements. The ionic radius of niobium is also closer to that of titanium. The influence of hydrothermal treatment temperature on the formation of titania solid solution nanoparticles co-doped with 20 mol% niobium and scandium was investigated. Fig. 1 shows XRD patterns of the precipitates formed from the precursor solution mixture of $Sc(NO_3)_3$, $TiOSO_4$, and $NbCl_5$ at starting composition ($X = 0.20$ in $Sc_XTi_{1-2X}Nb_XO_2$) under hydrothermal conditions at various temperatures of 100–210 °C for 5 h in the presence of urea. The crystalline phase of anatase was clearly detected in the precipitates as-prepared at the temperatures more than 120 °C although appearance of very broad peaks at the positions of anatase diffraction lines was observed in the sample after heat treatment at 100 °C. The precipitates obtained by hydrothermal treatment at 150–180 °C were detected as a single phase of anatase-type structure, and no trace of diffraction peaks due to another phase were detected. In the present study, precipitation temperature of nanocrystalline anatase from the precursor solution mixture under hydrothermal conditions at weakly basic conditions in the presence of urea was lower than that in the case of hydrothermal crystallization from amorphous co-precipitates prepared by dropping aqueous ammonia [19]. This result suggests that the hydrothermal treatment at temperature more than 180 °C is appropriate and necessary for obtaining anatse with nano-sized crystallite having sufficient crystallinity.

Fig. 2 shows the effect of hydrothermal treatment temperature on the crystallite size of anatase in as-prepared precipitates (starting $X = 0.20$ in $Sc_XTi_{1-2X}Nb_XO_2$) as a function of treatment temperature. The crystallite size was estimated from the XRD line broadening of 1 0 1 diffraction peak of anatase. The crystallite of anatase in the range of nanometric levels grew with increased

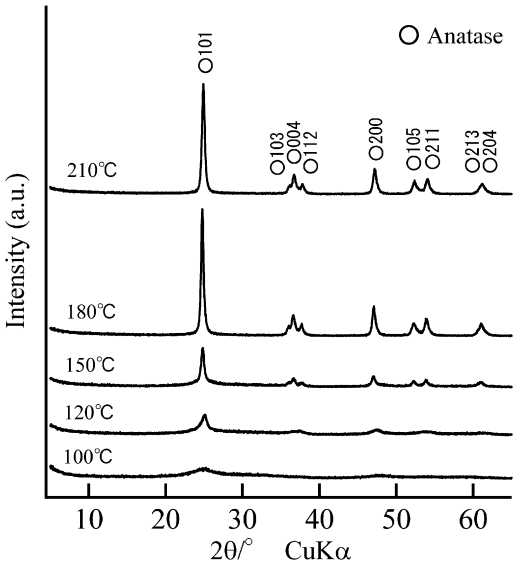

Fig. 1. X-ray diffraction patterns of precipitates obtained at starting composition of $X = 0.20$ in $Sc_XTi_{1-2X}Nb_XO_2$ under hydrothermal conditions at various temperatures of 100–210 °C for 5 h.

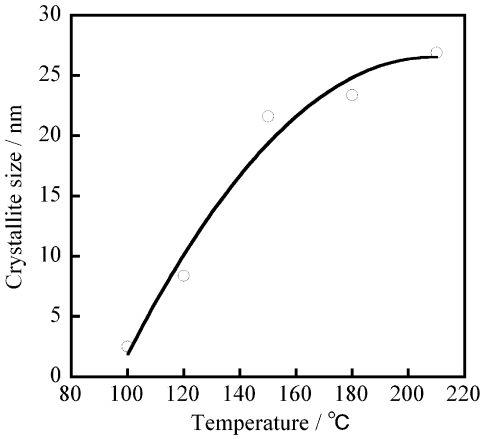

Fig. 2. Crystallite size of anatase-type precipitates as-prepared at starting composition of $X = 0.20$ in $Sc_XTi_{1-2X}Nb_XO_2$ under hydrothermal conditions for 5 h plotted against hydrothermal treatment temperature.

treatment temperature, although increase rate in size became gradually slow down. The effect of starting total metal cation concentration (Sc+Ti+Nb) of the precursor solution mixture on the crystallite size of anatase was investigated. The precipitates obtained from the precursor solution mixture with total metal cation concentration 0.1–0.5 mol/dm^3 under hydrothermal condition at 180 °C for 5 h were detected as single phase anatase-type structure without a trace of another diffraction

peaks. Fig. 3 shows the crystallite size of as-prepared anatase as a function of starting total cation concentration. Gradual increase in the crystallite size of anatase was observed with increased total cation concentration of the precursor solution mixture.

3.2. Anatase $Sc_XTi_{1-2X}Nb_XO_2$ with wide solid solution range

Fig. 4 shows XRD patterns of precipitates formed from precursor solution mixture with total metal cation concentration of 0.5 mol/dm^3 at various starting compositions ($X = 0$, and 0.20–0.40 in $Sc_XTi_{1-2X}Nb_XO_2$) under mild hydrothermal conditions at 180 °C for 5 h. The crystalline phase detected in all the as-prepared precipitates except the sample $X = 0.40$ was only a single phase of anatase. No diffraction peaks due to other crystalline phases were detected. In the sample $X = 0.40$ almost all diffraction lines were detected as anatase phase but unknown peaks with very slight intensity were detected. It is considered that this phenomenon may show the limit of the direct formation of a single phase of anatase-type solid solution under this hydrothermal condition. Since the sample $X = 0.40$ is not so uniform as other samples from the viewpoint of the existence of a small amount of unknown phase, we investigated the properties of the samples $X < 0.40$ with a single phase of anatase in this study.

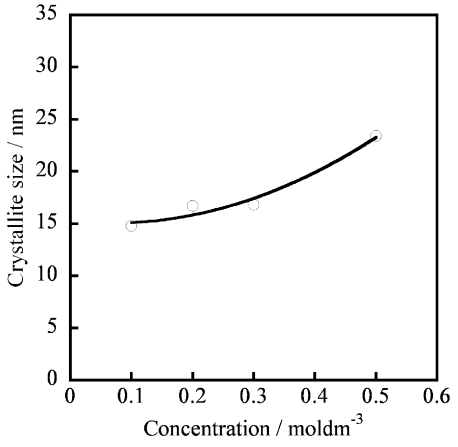

Fig. 3. Crystallite size of anatase-type precipitates as-prepared at starting composition of $X = 0.20$ in $Sc_XTi_{1-2X}Nb_XO_2$ under hydrothermal conditions at 180 °C for 5 h plotted against total metal cation concentration (Sc+Ti+Nb) of the precursor solution mixture.

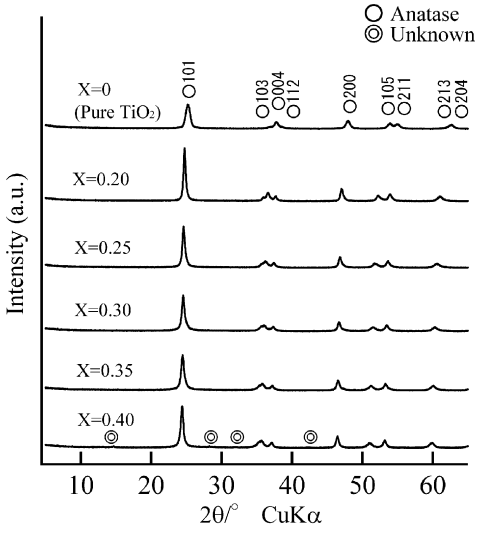

Fig. 4. X-ray diffraction patterns of precipitates formed at various starting compositions of $X = 0$ and 0.20–0.40 in $Sc_XTi_{1-2X}Nb_XO_2$ under hydrothermal conditions at 180 °C for 5 h.

It is important to analyze the chemical compositions of the resultant solid precipitates in order to discuss whether the compositions of the products coincide with the starting compositions of the samples or not. The analytical results of the chemical compositions of the resultant powders with a single phase of anatase are shown in Table 1, which were determined by the elemental analysis using an ICP emission spectrometer. The content of Ti in the analytical compositions of the as-prepared samples was slightly more than that in the starting compositions of the samples. We must also reconsider the reliability of the chemical quantitative analysis of water of crystallization (n value) associated in the starting material $TiOSO_4 \cdot nH_2O$, although consideration should also be given to the reliability of the ICP analysis. We showed analytical X values in Table 1 based on the analytical contents of Sc and Nb.

A gradual shift of the diffraction lines of the as-prepared anatase-type TiO_2 to a lower diffraction angle is observed with increased the value of X in Fig. 4. Then the lattice parameters a_0 and c_0 of the as-prepared anatase-type TiO_2 were plotted in Fig. 5 using analytical X values based on the analytical contents of Sc and Nb in Table 1 because it is difficult to plot the lattice parameters a_0 and c_0 of as-prepared anatase-type TiO_2 in accordance with individual values of the real Sc and Nb contents. Though the lattice parameters were plotted using analytical X values to confirm the formation of anatase-type solid solutions, we usually used the starting X values as representative X in this study. Linear increase in the lattice parameters a_0 and c_0 were observed with increased niobium and scandium content doped into TiO_2. The lattice parameter c_0 increased more than a_0.

The corresponding lattice parameter change and the gradual shift of the diffraction lines in the XRD patterns with increased the value of X indicated that the anatase-type solid solutions were formed by substituting for titanium sites by niobium (Nb^{5+} 0.64 Å) and scandium (Sc^{3+} 0.73 Å) with slightly larger ionic radii than that of titanium (Ti^{4+} 0.61 Å) [26]. Anatase-type solid solutions $Sc_XTi_{1-2X}Nb_XO_2$ with very wide solid solution range of $X = 0$–0.35 were directly formed as nanoparticles under hydrothermal

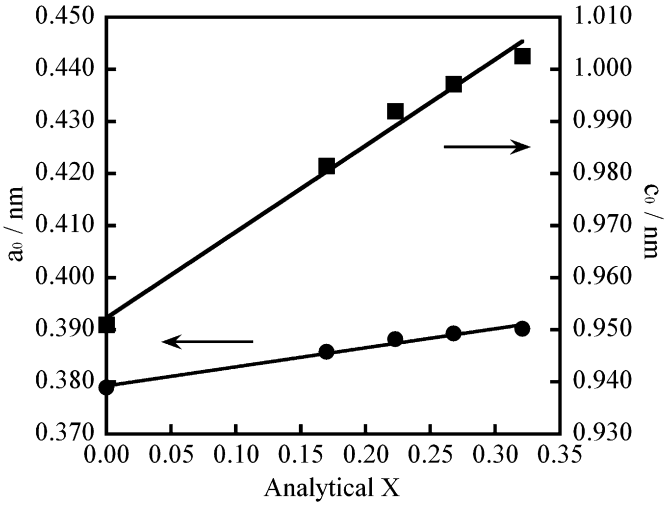

Fig. 5. Lattice parameters a_0 and c_0 of anatase-type $Sc_XTi_{1-2X}Nb_XO_2$ formed under hydrothermal conditions at 180 °C for 5 h.

conditions. There has been no information on the presence of anatase-type crystal in which titanium component is minor in the composition. This study must be the first report on the direct formation of anatase in which titanium component is minor in the composition. In Table 1, the analytical composition in the sample $Sc_XTi_{1-2X}Nb_XO_2$ solid solution with starting $X = 0.35$ is considered to be approximated by $Sc_{0.33}Ti_{0.33}Nb_{0.33}O_2$ ($= ScTiNbO_6$) composition in a certain degree although analytical X is 0.321. This is a single phase of anatase with composition $ScTiNbO_6$.

Fig. 6 shows TEM images of the as-prepared anatase-type $Sc_XTi_{1-2X}Nb_XO_2$ solid solutions. The particle size of anatase increased with increased niobium and scandium content in the composition. The crystallite size of anatase estimated from the XRD line broadening corresponded relatively well to the particle size of the samples estimated from the TEM observation.

The diffuse reflectance spectra of the as-prepared anatase-type $Sc_XTi_{1-2X}Nb_XO_2$ solid solutions are shown in Fig. 7. Slight and gradual shift of the onset of absorption to shorter wavelengths was observed with increased X value. The optical band gap is estimated using $\alpha h\nu = \text{const}\ (h\nu - E_g)^n$, where α is the absorption coefficient, $n = 1/2$ for a direct allowed transition, and $n = 2$ for an indirect allowed transition. Fig. 8 shows the band gap values for the anatase-type $Sc_XTi_{1-2X}Nb_XO_2$ solid solutions as a function of the analytical X, which were determined from the energy intercept by extrapolating the straight regions of the plot of $(\alpha h\nu)^2$ versus the photon energy $h\nu$ for a direct allowed transition

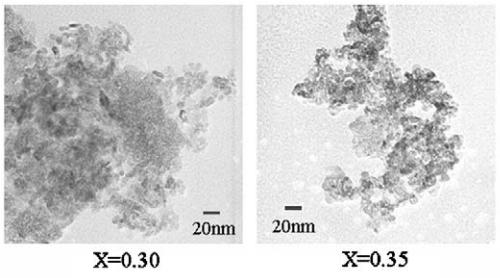

Fig. 6. Transmission electron microscopic images of precipitates with various compositions of (a) $X = 0.30$ and (b) 0.35 in $Sc_XTi_{1-2X}Nb_XO_2$ obtained under hydrothermal conditions at 180 °C for 5 h.

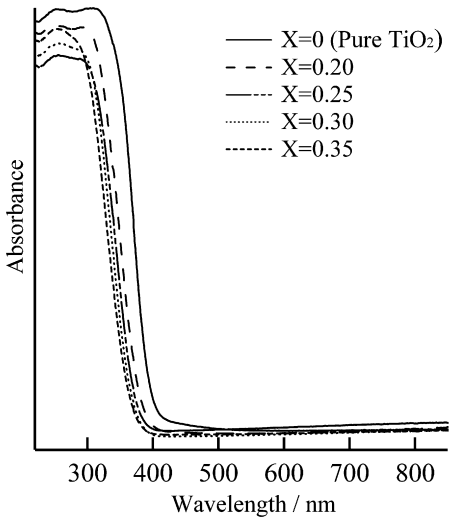

Fig. 7. Diffuse reflectance spectrum of as-prepared anatase-type solid solutions with various compositions of $X = 0$ and 0.20–0.35 in $Sc_XTi_{1-2X}Nb_XO_2$ prepared under hydrothermal conditions at 180 °C for 5 h.

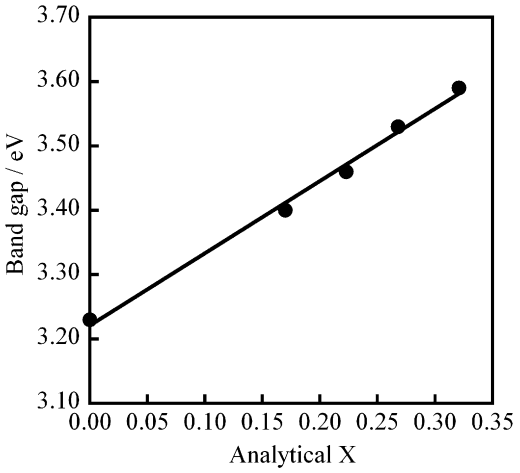

Fig. 8. Optical bang gap of as-prepared anatase-type solid solutions with various compositions in $Sc_XTi_{1-2X}Nb_XO_2$ prepared under hydrothermal conditions at 180 °C for 5 h.

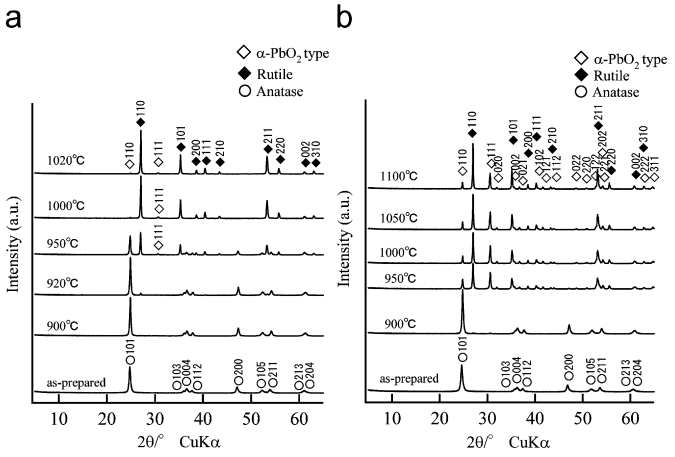

Fig. 9. X-ray diffraction patterns of samples with starting composition of (a) $Sc_{0.20}Ti_{0.60}Nb_{0.20}O_2$ and (b) $Sc_{0.25}Ti_{0.50}Nb_{0.25}O_2$ before and after heating at 900–1100 °C for 1 h.

(E_d). The optical band gap value of anatase almost linearly and gradually increased when the value of X was increased, i.e. with increased niobium and scandium content co-doped in the sample.

3.3. Phase stability of anatase and formation of α-PbO_2 phase

In the previous work, the XRD patterns of the $Sc_XTi_{1-2X}Nb_XO_2$ solid solutions with compositions $X = 0.15$ before and after heating at 900–1000 °C for 1 h showed that the anatase-type $Sc_{0.15}Ti_{0.70}Nb_{0.15}O_2$ solid solution transformed into a resultant single phase of new rutile-type $Sc_{0.15}Ti_{0.70}Nb_{0.15}O_2$ solid solution without a trace of diffraction peaks due to another phase [21]. The XRD patterns of the $Sc_XTi_{1-2X}Nb_XO_2$ solid solutions with compositions $X = 0.20$ and 0.25 before and after heating at 900–1050 °C for 1 h are shown in Fig. 9(a) and (b), respectively. By heating, anatase-to-rutile phase transition began at 920 °C and concluded at 1000 °C, and rutile solid solution phase with a trace of diffraction peaks of α-PbO_2 phase was formed in the $Sc_{0.20}Ti_{0.60}Nb_{0.20}O_2$ sample. With increase in the atomic fraction replaced by niobium and scandium, the ratio of α-PbO_2 phase increased in the solid solution consisting of rutile and α-PbO_2 phase after phase transformation as shown in Fig. 9(b).

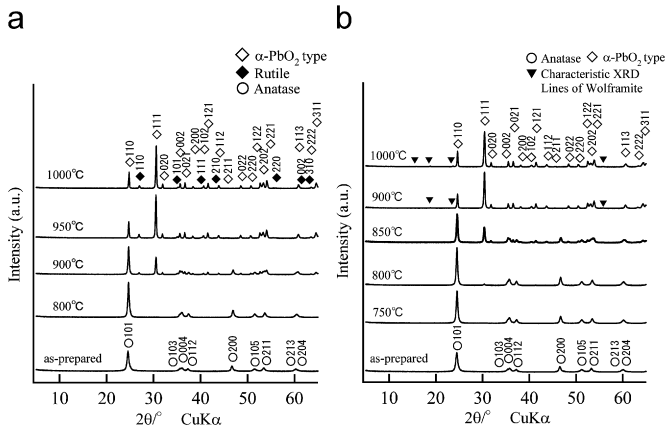

Fig. 10. X-ray diffraction patterns of samples with starting composition of (a) $Sc_{0.30}Ti_{0.40}Nb_{0.30}O_2$ and (b) $Sc_{0.35}Ti_{0.30}Nb_{035}O_2$ before and after heating at 750–1000 °C for 1 h.

Phase transformation behavior of anatase-type $Sc_XTi_{1-2X}Nb_XO_2$ solid solutions with compositions starting $X = 0.30$ and 0.35 are shown in Fig. 10(a) and (b), respectively. The fraction of α-PbO_2 phase fairly increased in the solid solution with starting $X = 0.30$ after phase transformation in comparison with the sample with starting $X = 0.25$ (Fig. 9(b)). Through anatase-to-α-PbO_2 phase transformation, almost completely single phase of orthorhombic α-PbO_2 without a trace of diffraction peaks of rutile but with an extremely small intensity of unidentified diffraction peaks was formed at 900–1000 °C in the sample with starting $X = 0.35$ (Fig. 10(b)).

Pure titania can also exist as orthorhombic α-PbO_2 structure under high pressure besides three distinct polymorphs: rutile, anatase, and brookite [22–25]. The appearance of orthorhombic α-PbO_2 structure under mechanical activation through high energy ball milling and ambient pressure has been observed in the mixture of TiO_2 and graphite [27], nanocrystalline TiO_2 powders [28], and Fe-doped TiO_2 [29]. The α-PbO_2 phase is also one of the structures appeared as srilankite in the binary system ZrO_2–TiO_2 [30–33]. There are many compounds with α-PbO_2 or α-PbO_2 related structure as mentioned above and as MWO_4 (M: Cd, Mg, Co, Ni, Fe, Mn, Zn), $MM'O_4$ (M: Sc, In, M': Nb, Ta), $HfTiO_4$, $ZrSnO_4$, etc. Exclusive of high pressure modification α-PbO_2 phase of TiO_2 [22–24] and $ScNbO_4$ [34], few reports could be found on the synthesis of compound having composition $ScTiNbO_6$ with α-PbO_2 or α-PbO_2 related structure in the ternary system Sc_2O_3–TiO_2–Nb_2O_5.

The high pressure TiO_2 modification, orthorhombic srilankite, which has α-PbO_2 structure with disorderd cations. On the other hand, the compound $ScNbO_4$ has monoclinic wolframite-type structure, which is ordered one based on α-PbO_2 [35]. In dimensions, the monoclinic wolframite with ordered structure based on α-PbO_2 is very similar to orthorhombic structure with disorderd one. Although the sample after heat treatment at 900 °C is identified as orthorhombic α-PbO_2 structure, unidentified diffraction peaks with extremely small intensity are detected in Fig. 10(b). These unidentified diffraction peaks perfectly correspond to a part of characteristic XRD lines of monoclinic wolframite $ScNbO_4$. However, it is not adequate to identify as monoclinic wolframite structure because the intensity of these unidentified diffraction peaks was very much low as monoclinic symmetry of wolframite. The phase appeared after heat treatment at 900–1000 °C is considered to be α-PbO_2 structure with possibly some cation order similar to that seen in wolframite

As shown in Fig. 10(b), we have found the presence of a compound with α-PbO_2 structure in the ternary system Sc_2O_3–TiO_2–Nb_2O_5. In Table 1, the analytical composition in the sample $Sc_XTi_{1-2X}Nb_XO_2$ solid solution with starting $X = 0.35$ is considered to be approximated by $Sc_{0.33}Ti_{0.33}Nb_{0.33}O_2$ ($= ScTiNbO_6$) in a certain degree. Thus, the compound $ScTiNbO_6$ that was almost completely single phase of α-PbO_2 structure with possibly some cation order similar to that seen in wolframite was synthesized through heat treatment at 900 °C in air via phase transformation from anatase-type titania solid solution.

3.4. Photocatalytic activity of $Sc_XTi_{1-2X}Nb_XO_2$

The influence of the niobium and scandium content on the adsorptivity and photocatalytic activity for the as-prepared anatase samples having the value of starting X and reference pure TiO_2 powder ST-01 (anatase-type structure, BET specific surface area: 302 m^2/g, crystallite size: 7 nm, Ishihara Sangyo Kaisha Ltd., Osaka, Japan) as changes in the concentration of MB with time in the dark and under UV-light irradiation was investigated. The photocatalytic activity of as-prepared anatase samples is shown in Fig. 11 as plots of $-\ln(C/C_0)$ versus UV-light irradiation time. The plots gave almost straight lines, which suggest that the photocatalytic decomposition of MB follows pseudo-first-order kinetics with respect to MB concentration. The slope of the straight lines in Fig. 11 shows photocatalytic activity. The photocatalytic activity of pure anatase-type TiO_2 formed under this hydrothermal condition was relatively good in comparison with the reference sample ST-01. In the previous report [21], the anatase-type $Sc_XTi_{1-2X}Nb_XO_2$ with $X = 0.05$ showed nearly two times and three times as high photocatalytic activity as those of the hydrothermal anatase-type pure TiO_2 and commercially available reference pure TiO_2 (ST-01), respectively. The slope of the straight lines of anatase $Sc_XTi_{1-2X}Nb_XO_2$ with $X > 0.25$ became gradually gentle with increased niobium and scandium content. The sample with $X = 0.35$ showed the lowest photocatalytic activity. Anatase-type solid solutions that were doped with niobium and scandium and directly formed under hydrothermal conditions had effective photocatalytic activity, but the addition of excessive amount of dopants resulted in a reduction of the total photoactivity, partly because of the decrease of photoactive TiO_2 content in the sample.

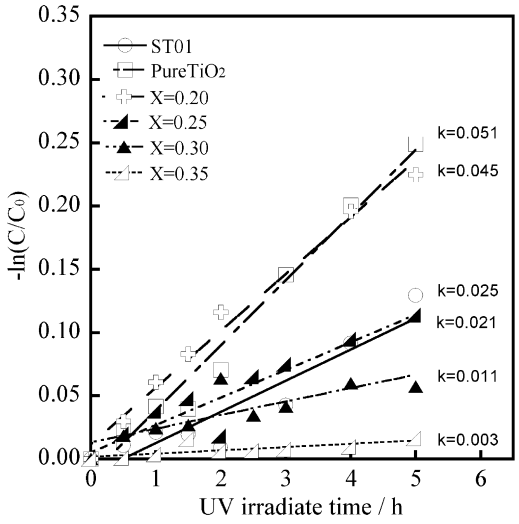

Fig. 11. Photocatalytic degradation of methylene blue as a function of ultraviolet irradiation time for reference sample ST-01 and as-prepared anatase-type solid solutions with various compositions of $X = 0$ and 0.20–0.35 in $Sc_XTi_{1-2X}Nb_XO_2$.

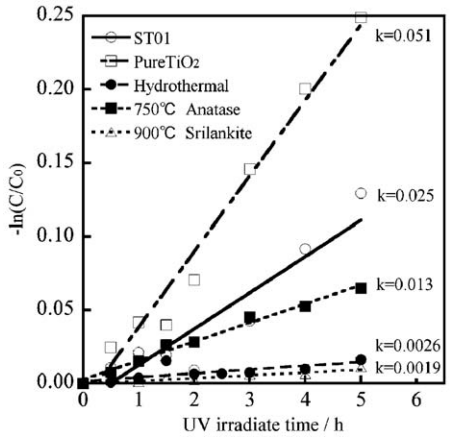

Fig. 12. Photocatalytic degradation of methylene blue as a function of ultraviolet irradiation time for reference sample ST-01, as-prepared anatase-type titania with composition of pure TiO_2 and $Sc_{0.35}Ti_{0.30}Nb_{035}O_2$, anatase-type $Sc_{0.35}Ti_{0.30}Nb_{035}O_2$ after heat treated at 750 °C, and α-PbO_2 phase of $Sc_{0.35}Ti_{0.30}Nb_{035}O_2$ formed at 900 °C.

Table 2
Lattice parameters, band gap, and BET surface area of as-prepared anatase-type $ScTiNbO_6$ and α-PbO_2 phase of $ScTiNbO_6$ after heat treatment at 1000 °C for 1 h.

Sample	Lattice parameter (nm)			Band gap (eV)	BET surface area (m^2/g)
	a_0	b_0	c_0		
Anatase-type	0.3902	–	1.0026	3.59	110
α-PbO_2 phase	0.4714	0.5631	0.5045	3.58	15

The effect of heat treatment in air i.e. calcination on the photocatalytic activity of the samples with anatase and α-PbO_2 phase having $ScTiNbO_6$ composition was investigated. Fig. 12 shows photocatalytic activity as plots of $-\ln(C/C_0)$ versus UV-light irradiation time. The photocatalytic activity of anatase-type $ScTiNbO_6$ as-prepared under hydrothermal condition was enhanced via heat treatment at 750 °C though it was lower than that of anatase samples with pure TiO_2 composition. The α-PbO_2 phase obtained after heat treatment at 900 °C through phase transformation showed low activity because of low surface area.

In the present study, anatase $Sc_XTi_{1-2X}Nb_XO_2$ with wide solid solution range ($X = 0$–0.35), anatase-type $ScTiNbO_6$, and α-PbO_2-type $ScTiNbO_6$ were formed. We summarize the data on the lattice parameters, band gap, and specific surface area of anatase-type and α-PbO_2-type $ScTiNbO_6$ in Table 2.

4. Summary

Anatase-type $Sc_XTi_{1-2X}Nb_XO_2$ solid solutions with wide solid solution range ($X = 0$–0.35) were hydrothermally formed as nanoparticles from the precursor solutions of $Sc(NO_3)_3$, $TiOSO_4$, $NbCl_5$ at 180 °C for 5 h using the hydrolysis of urea. The lattice parameters a_0 and c_0 and optical band gap value of anatase gradually increased with increase in the value of X. The α-PbO_2 phase which appeared in addition to rutile one in the sample with starting $X > 0.20$ after phase transformation increased in proportion when the value of X was increased. The solid solutions in the range $0.20 <$ starting $X < 0.35$ were composed of multiphase α-PbO_2+rutile after phase transformation. The fraction of α-PbO_2 phase in the solid solution with starting $X = 0.30$ after phase transformation fairly increased in comparison with the sample with starting $X = 0.25$. A compound $ScTiNbO_6$ ($Sc_{0.33}Ti_{0.33}Nb_{0.33}O_2$) that was identified as a closely single phase of α-PbO_2 with a trace of symptomatic wolframite α-PbO_2 related structure was formed at 900–1000 °C.

References

[1] T. Kasuga, M. Hiramatsu, A. Hoson, T. Sekino, K. Niihara, Langmuir 14 (1998) 3160–3163.
[2] W.J. Dawson, Am. Ceram. Soc. Bull. 67 (1988) 1673–1678.
[3] S. Komarneni, Current Sci. 85 (2003) 1730–1734.
[4] M. Hirano, M. Inagaki, J. Mater. Chem. 10 (2000) 473–477.
[5] M. Hirano, T. Miwa, M. Inagaki, J. Am. Ceram. Soc. 84 (2001) 1728–1732.
[6] M. Hirano, J. Mater. Chem. 10 (2000) 469–472.
[7] M. Hirano, N. Sakaida, J. Am. Ceram. Soc. 85 (2002) 1145–1150.
[8] M. Hirano, H. Morikawa, M. Inagaki, M. Toyoda, J. Am. Ceram. Soc. 85 (2002) 1915–1920.
[9] M. Hirano, H. Morikawa, Chem. Mater. 15 (2003) 2561–2566.
[10] A. Fujishima, T.N. Rao, D.A. Tryk, J. Photochem. Photobiol. C Photochem. Rev. 1 (2000) 1–21.
[11] A.W. Czanderna, C.N.R. Rao, J.M. Honig, Trans. Faraday Soc. 54 (1958) 1069–1073.
[12] S.R. Yoganarasimhan, C.N.R. Rao, Trans. Faraday Soc. 58 (1962) 1579–1589.
[13] M. Hirano, T. Joji, M. Inagaki, H. Iwata, J. Am. Ceram. Soc. 87 (2004) 35–41.
[14] M. Hirano, C. Nakahara, K. Ota, M. Inagaki, J. Am. Ceram. Soc. 85 (2002) 1333–1335.
[15] M. Hirano, C. Nakahara, K. Ota, O. Tanaike, M. Inagaki, J. Solid State Chem. 170 (2003) 39–47.
[16] M. Hirano, K. Ota, T. Ito, J. Am. Ceram. Soc. 88 (2005) 3303–3310.
[17] M. Hirano, K. Matsushima, J. Am. Ceram. Soc. 89 (2006) 110–117.
[18] M. Hirano, K. Matsushima, J. Nanosci. Nanotechnol. 6 (2006) 762–770.
[19] M. Hirano, K. Date, J. Am. Ceram. Soc. 88 (2005) 2604–2607.
[20] M. Hirano, T. Ito, J. Nanosci. Nanotechnol. 6 (2006) 3820–3827.
[21] M. Hirano, T. Ito, Mater. Res. Bull. 43 (2008) 2196–2206.
[22] R.K. Linde, P.S. De Carli, J. Chem. Phys. 50 (1969) 319–325.
[23] N.A. Bendeliani, S.A. Popova, L.F. Vereschchagin, Geokhimiya (1966) 499–501.
[24] J. Haines, J.M. Leger, Physica B 192 (1993) 233–237.
[25] H. Sato, S. Endo, M. Sugiyama, T. Kikegawa, O. Shimomura, K. Kusaba, Science 251 (1991) 786–788.
[26] R.D. Shannon, Acta Cryst. A 32 (1976) 751–767.
[27] R. Ren, Z. Yang, L.L. Shaw, J. Mater. Sci. 35 (2000) 6015–6026.
[28] X. Pan, X. Ma, J. Solid State Chem. 177 (2004) 4098–4103.
[29] D.-M. Jiang, X.-Y. Pan, W.-Z. Shi, X.-M. Ma, J. Shanghai Univ. 10 (2006) 161–164.
[30] A. Willgallis, E. Siegmann, T. Hettiaratchi, Neues Jahrb. Mineral. Monatsh. (1983) 151–157.
[31] A.E. McHale, R.S. Roth, J. Am. Ceram. Soc. 69 (1986) 827–832.
[32] J.C. Buhl, A. Willgallis, Cryst. Res. Tech. 24 (1989) 263–268.
[33] R. Merkle, H. Bertagnolli, J. Mater. Chem. 8 (1998) 2433–2439.
[34] C. Keller, Z. fuer Anorg. und Allg. Chem. 318 (1962) 89–106.
[35] J. Graham, M.R. Thornber, Am. Mineralogist 59 (1974) 1026–1039.